ANTIMICROBIAL AGENTS AND CHEMOTHERAPY, Mar. 2002, p. 787–796 Vol. 46, No. 3
0066-4804/02/$04.00+0 DOI: 10.1128/AAC.46.3.787–796.2002

Relationship between Chloroquine Toxicity and Iron Acquisition in *Saccharomyces cerevisiae*

Lyndal R. Emerson,[1] Martin E. Nau,[2] Rodger K. Martin,[3] Dennis E. Kyle,[3] Maryanne Vahey,[4] and Dyann F. Wirth[1]*

Department of Immunology and Infectious Diseases, Harvard School of Public Health, Boston, Massachusetts[1]; Henry M. Jackson Foundation for the Advancement of Military Medicine, Rockville, Maryland[2]; and Division of Experimental Therapeutics[3] and Division of Retrovirology,[4] Walter Reed Army Institute of Research, Washington, D.C.

Received 30 May 2001/Returned for modification 6 June 2001/Accepted 20 November 2001

Chloroquine is one of the most effective antimalarials, but resistance to it is becoming widespread. However, we do not fully understand either the drug's mode of action or the mechanism of resistance. In an effort to expand our understanding of the mechanism of action and resistance associated with chloroquine, we used *Saccharomyces cerevisiae* as a model eukaryotic system. To aid in the discovery of potential drug targets we applied the transcriptional profiling method to identify genes transcriptionally responsive to chloroquine treatment in *S. cerevisiae*. Among the genes that were differentially expressed with chloroquine treatment were a number of metal transporters involved in iron acquisition (*SIT1*, *ARN2*, *ARN4*, and *SMF2*). These genes exhibit similar expression patterns, and several are known to be regulated by AFT1, a DNA binding protein, which responds to iron levels in the cell. We investigated the role of chloroquine in iron metabolism by using a variety of approaches, including pharmacological, genetic, and biochemical techniques. For these experiments, we utilized yeast lacking the major iron uptake pathways (*FET3* and *FET4*) and yeast deficient in *SIT1*, encoding the major up-regulated iron siderophore transporter. Our experiments show that yeast genetically or environmentally limited in iron availability has increased sensitivity to chloroquine in pharmacological assays and that the addition of iron rescues these cells from chloroquine killing. $^{55}FeCl_3$ accumulation was inhibited in the presence of chloroquine, and kinetic analysis demonstrated that inhibition was competitive. These results are consistent with deprivation of iron as a mechanism of chloroquine killing in yeast.

Chloroquine (CQ) is commonly used for treatment of malaria; however, its mode of action and the mechanism of resistance are still not fully understood. Better knowledge of CQ's mode of action may make it possible to identify new drugs that target similar pathways or to reverse existing resistant phenotypes.

CQ has been shown to interact in both mammalian cells and *Plasmodium* spp. with a number of different pathways, including changes in vacuolar (or lysosomal) pH (9, 22, 39, 56), binding to DNA and RNA (3, 11, 41, 53), binding to heme and β-hematin in *Plasmodium falciparum* (1, 55; reviewed in reference 20). In the case of *P. falciparum*, CQ was an effective drug whose efficacy has been severely compromised by the emergence of drug-resistant parasites (8, 20).

To analyze the mechanism of CQ action, we used transcriptional profiling in a model eukaryotic system, *Saccharomyces cerevisiae*. Differential transcriptional profiling using microarray analysis is based on detecting differences in expression of mRNAs in cells treated under different conditions. No information other than the genomic sequence and the open reading frame (ORF) predictions is necessary to assay mRNA expression. Such whole-genome analysis allows the determination of expression profiles without preselection of genes. For the experiments described here, we used the Affymetrix Yeast Chip YE6100, which is based on the oligonucleotide array method. We published the adaptation of this system to the wild-type *S. cerevisiae* strain YPH499 and derivatives previously (38).

From this transcriptional profile analysis, we identified a number of genes whose products are involved in metal acquisition and metabolism that have increased mRNA levels during challenge with CQ. Increased expression of genes involved in iron (Fe) availability suggested that CQ toxicity might, in part, result from interference with iron uptake or metabolism. Although CQ has been demonstrated to disrupt iron trafficking in several cell types, including pathogenic yeasts (9, 22, 39), the observation of altered expression of iron metabolism genes in *S. cerevisiae* was surprising. In all these cases, CQ disrupts iron trafficking by increasing pH in lysosomes and preventing the release of iron from the carrier proteins. No iron carrier protein system has been identified in *S. cerevisiae*, and thus, this mechanism of CQ action is very unlikely in *S. cerevisiae*. Therefore, we initiated a more thorough investigation of genes involved in metal transport and availability, with particular interest in those involved with iron transport.

In this study, we investigated the role of CQ in iron trafficking using a variety of approaches involving pharmacological, genetic, and biochemical techniques. One of the advantages of the *S. cerevisiae* system is the availability not only of the whole genome sequence but also of mutants deficient in specific genes or combinations of genes, thus allowing genetic dissection of pathways. For these experiments, we utilized yeast lacking the major iron uptake pathways (*Fet3* and *Fet4*) as well as yeast deficient in *SIT1*, the major iron siderophore transporter that is induced under CQ pressure.

* Corresponding author. Mailing address: Department of Immunology and Infectious Diseases, Harvard School of Public Health, 665 Huntington Ave., Boston, MA 02115. Phone: (617) 432-1563. Fax: (617) 432-4766. E-mail: dfwirth@hsph.harvard.edu.

MATERIALS AND METHODS

Strains and media. The following strains of *S. cerevisiae* were used: YPH499 (*MAT***a** *ade2-101*oc *his3Δ200 leu2-Δ1 lys2-801*am *trp1-Δ1 ura3-52*), DEY1455 (*MAT*α *ade2 can1 his3 leu2 trp1 ura3 gal*), DEY1455ΔSIT1 (*MAT*α *ade2 can1 his3 leu2 trp1 ura3 gal SIT1*::KanM), DEY1433 (*MAT*α *ade2 can1 his3 leu2 trp1 ura3 FET3*::*HIS3 FET4*::*LEU2*), and DEY1433ΔSIT1 (*MAT*α *ade2 can1 his3 leu2 trp1 ura3 FET3*::*HIS3 FET4*::*LEU2 SIT1*::KanM) (31, 32). Unless otherwise stated, cells were grown in YPAD (yeast-peptone-adenine-dextrose) medium or on YPAD agar. Low-iron medium minus EDTA (LIM−EDTA) was prepared by the protocols of Eide et al. (17, 18).

Preparation, assay, and analysis of mRNA populations. The following methods were described in detail by Nau et al. (38). In brief, CQ (3 and 5 mM)-treated and control cultures were harvested at 2 and 3 h, and total RNA was extracted using 400-μm acid-washed glass beads and Tri-Reagent per the manufacturer's instructions (Molecular Research Center, Woodlands, Tex.). Poly(A) RNA (mRNA) was prepared from total RNA by the Oligotex method according to the manufacturer's instructions (Qiagen, Chatsworth, Calif.). Double-stranded cDNA was synthesized in two steps with the Superscript Choice system (Gibco-BRL, Rockville, Md.) and the reverse transcription primer T7-$(dT)_{24}$ [5′GGCC AGTGAATTGTAATACGACTCACTATAGGGAGGCGG-$(dT)_{24}$] (Genset Corp., La Jolla, Calif.). Synthesis of biotin-labeled cRNA was carried out by in vitro transcription with a MEGAscript T7 in vitro transcription kit (Ambion, Inc.), following the manufacturer's instructions. The biotin-labeled cRNA was purified on Qiagen RNeasy spin columns (Qiagen, Valencia, Calif.) following the manufacturer's protocol, fragmented in a 40-μl reaction mixture containing 40 mM Tris-acetate (pH 8.1), 100 mM potassium acetate, and 30 mM magnesium acetate, and incubated at 94°C for 35 min. The biotin-labeled and fragmented cRNA was hybridized to the YE6100 yeast GeneChip array (Affymetrix, Santa Clara, Calif.) following the manufacturer's instructions. GeneChip arrays were stained for 15 min at room temperature and at 60 rpm with streptavidin-phycoerythrin (Molecular Probes, Inc., Eugene, Oreg.) stain solution at a final concentration of 10 μg/ml in 6× SSPE (1× SSPE is 0.18 M NaCl, 10 mM NaH_2PO_4, and 1 mM EDTA [pH 7.7])-T buffer and 1.0 mg of acetylated bovine serum albumin (Sigma, St. Louis, Mo.)/ml.

GeneChip arrays were scanned with an HP GeneArray scanner (Hewlett-Packard, Santa Clara, Calif.) controlled by GeneChip 3.1 software (Affymetrix). A value of 3.0-fold was selected as the cutoff for a conservative first-pass analysis of changes in expression. Values of 2-fold or greater are generally accepted as reliable with this system per the manufacturer's specifications and empirical evaluation (10, 59). All values above the 3.0-fold cutoff were included in the initial analysis of experimental expression profiles. In later analyses, values of 2-fold or above were included for comparative purposes and to expand observation of groups of interest. The untreated control was used as a baseline for comparison to the treated strain in all cases.

Bioinformatic analyses. GeneSpring version 3.0 (Silicon Genetics, San Carlos, Calif.) was used to derive global trends in the expression profiles and to specifically assess the expression patterns of the metal transporter gene targets. For the temporal analysis, the raw data from the Affymetrix platform were normalized as described by Nau et al. (38) and reported as the change between the treatment and the control. The data were clustered by self-organizing maps and K-mean methods based on similarities in expression profiles. K-mean clustering is a top-down method that starts with a collection of items and some chosen number of clusters (k). In the present study, the optimum value for k was determined to be 6 after assessment of a range of possible k values to find a number of groupings that allowed distribution of profiles into reasonable categories. The clustering proceeds by repeated iterations of a two-step process where the mean vector for all items in each cluster is computed and items are reassigned to the cluster whose center is closest to the item. Self-organizing maps is a method of clustering similar to K-mean clustering with some additional constraints imposing more partial structure on the clusters. In our hands, these two methods produced very similar results, possibly in part due to the relatively simple structure of our temporal data set. The final clusters presented in this work are standard correlation K-mean derived with final assignments confirmed by hand.

Northern slot blot analysis. Total RNA was isolated from CQ-treated and control cells as described above. A dilution series of total RNA (3.25, 7.5, 15, 30, and 60 μg) for each sample was applied to Hybond-N+ positively charged nylon membranes (Amersham Pharmacia Biotech, Piscataway, N.J.) using a Bio-Dot SF microfiltration apparatus (Bio-Rad, Hercules, Calif.) according to the manufacturer's directions. The resulting blots were probed with PCR-amplified labeled ORFs (Research Genetics, Huntsville, Ala.) in ULTRAhyb hybridization solution (Ambion, Austin, Tex.) according to the manufacturer's instructions and standard methods (48). Probe hybridization signals were measured with Image imaging software (National Institutes of Health, Bethesda, Md.).

Drug gradient challenge assay. Gradient plates, which contained an increasing concentration of drug (CQ or bathophenanthroline-disulfonic acid [BPS]) across the width of a 100- by 15-mm square petri dish, were made with YPAD medium containing 2% agar as previously described (12, 36). The edge of a sterile glass slide was used to transfer stationary-phase *S. cerevisiae* mixed 1:2 with molten agar (55°C) from a sterile surface to the drug gradient plate. In this manner, cells were spread uniformly across the gradient and between samples. The extent of cell growth across the gradient was determined after allowing 2 to 3 days' growth at 30°C. For assays involving the depletion of iron in the agar medium, BPS at 20 μM was added to both pours of YAPD agar to create a continuous concentration of BPS throughout the plate. For assays involving supplementation with iron, $FeCl_3$ prepared in 0.1 M HCl was added to both pours of YPAD agar to give the desired continuous concentration. For assays involving supplementation with copper, $CuSO_4$ prepared in 0.1 M HCl was added to both pours of YPAD agar to give the desired continuous concentration.

^{55}Fe accumulation assay. The protocol for iron transport studies was adapted from the work of Eide et al. (17, 18). Exponentially growing cells were centrifuged at 1,000 × *g* for 5 min at 4°C and washed twice in ice-cold assay buffer (LIM−EDTA). Washed cells were then resuspended in approximately 1/100 of the original volume in assay buffer and kept on ice until use. Uptake assay solutions were prepared by diluting $^{55}FeCl_3$ into chilled assay buffer to the desired concentration. To measure uptake, 50 μl of cell suspension was added to 450 μl of uptake assay buffer and incubated at 30°C for 360 min. The assay samples were then chilled on ice, vortexed, vacuum filtered through Whatman GF/C filters, and washed with 10 ml of ice-cold SSW (1 mM EDTA, 20 mM Na_3 citrate [pH 4.2], 1 mM KH_3PO_4, 1 mM $CaCl_2$, 5 mM $MgSO_4$, 1 mM NaCl). Cell-associated ^{55}Fe was measured with a Beckman LS5000TD liquid scintillation system. Nonspecific uptake due to cell surface absorption was determined by preparing parallel assay mixtures that were incubated on ice for 360 min before filtration and washing. For assays involving uptake of iron in the presence of CQ, $C_{18}H_{26}ClN_3 \cdot 2H_3PO_4$ prepared in distilled-deionized water was added to the desired concentration.

[^{14}C]CQ uptake assay. The quinoline–[3-^{14}C]CQ ([^{14}C]CQ) uptake assay protocol is a variation on the CQ uptake assay described by Krogstad et al. for *P. falciparum* and the Fe uptake assay described by Eide et al. for *S. cerevisiae* (17, 29). Exponentially growing cells were centrifuged at 1,000 × *g* for 5 min at 4°C and then resuspended in approximately 1/100 of the original volume in assay buffer (YPAD) and kept on ice until use. Uptake assay solutions were prepared by diluting [^{14}C]CQ) in chilled assay buffer to a concentration of 3 nM. To measure uptake, 50 μl of cell suspension was added to 450 μl of uptake assay buffer and incubated at 30°C for 5 to 30 min. The assay samples were then chilled on ice, vortexed, vacuum filtered through Whatman GF/C filters, and washed with 10 ml of ice-cold double-distilled H_2O. Cell-associated [^{14}C]CQ was measured with a Beckman LS5000TD liquid scintillation system.

Nonspecific uptake due to cell surface adhesion was determined by preparing parallel assay mixtures that were incubated on ice for 20 min before filtration and washing. For assays involving iron competition, $FeCl_3$ prepared in 0.1 M HCl was added to the desired concentrations.

Lineweaver-Burk plots. In order to determine the nature of the inhibition of iron uptake caused by CQ, we measured iron uptake over a range of iron substrate ($^{55}FeCl_3$) concentrations (0.1 to 10.0 μM). From these data we determined the Michaelis constant (K_m) and the maximal rate (V_{max}) by using the formula $1/V = 1/V_{max} + K_m/V_{max} \cdot 1/[S]$, where V is velocity and S is substrate.

Plotting $1/V$ versus $1/[S]$ yields a straight line with an intercept of $1/V_{max}$ and a slope of K_m/V_{max}. This plot gives the apparent K_m of $^{55}FeCl_3$ uptake for *S. cerevisiae* under normal conditions. This was repeated with CQ treatment (9.7 and 97 mM), and the structure of the resulting multiline plot was compared to plots of model competitive and noncompetitive inhibitors. From these data we calculated the dissociation constant of the inhibitor by the formulas $y = Mx + B$, where M is slope and B is the y intercept, and $(\text{slope}_{\text{normal}})\ (1 + [I]/K_i) = \text{slope}_{\text{inhibitor}}$.

RESULTS

Analysis of highly differential genes reveals shared response profile of several metal metabolism genes. We compared the expression profiles of CQ-treated yeast cells with untreated cells at 2 and 3 h. A total of 425 ORFs with an expression differential of ≥2-fold reported by the GeneChip were placed

TABLE 1. Genes with similar temporal expression organized by functional family groups[a]

Change (fold)		ORF	Protein name	Function	Family grouping
2 h	3 h				
1.1	9.8	YNL056W	BZR1	Similar to resistance protein	Detoxification and transport facilitation
1.7	6.0	**YEL065W**	**SIT1**	**Iron siderophore transporter**	**Detoxification and transport facilitation**
2.0	4.2	**YHL047C**	**ARN2**	**Iron siderophore transporter**	**Detoxification and transport facilitation**
1.7	3.9	**YOL158C**	**ARN4**	**Iron siderophore transporter**	**Detoxification**
−1.1	3.4	YDR538W	PAD1	Phenylacrylic acid decarboxylase	Detoxification
2.3	3.1	YNL239W	LAP3	Aminopeptidase	Detoxification
1.5	2.9	**YOR079C**	**ATX2**	**Metal chaperone**	**Detoxification**
1.5	4.8	YOR306C		Monocarboxylate transporter	Transport facilitation
2.4	3.0	YOR273C		Similar to resistance protein	Transport facilitation
1.6	3.0	YOL130W	ALR1	Divalent cation transporter	Transport facilitation
1.0	3.7	**YHR175W**	**CTR2**	**Copper transporter**	**Transport facilitation**
1.2	3.0	**YMR058W**	**FET3**	**Ferroxidase**	**Transport facilitation**
−1.4	34.4	YDL130W	RPP1B	Ribosomal protein	Protein synthesis
−1.1	33.6	YBR189W	RPS9B	Ribosomal protein	Protein synthesis
1.2	25.1	YLL045C	RPL8B	Ribosomal protein	Protein synthesis
−1.1	22.3	YOL127W	RPL25	Ribosomal protein	Protein synthesis
−1.4	16.5	YDL083C	RPS16B	Ribosomal protein	Protein synthesis
7.5	9.6	YGL032W	GLS2	Glucan synthase	Carbohydrate metabolism
1.2	8.8	YNL066W	SUN4	Beta-glucosidase	Carbohydrate metabolism
2.3	6.3	YOL126C	MDH2	Malate dehydrogenase	Carbohydrate metabolism
2.3	5.9	YDL022W	GPD1	Dehydrogenase	Carbohydrate metabolism
1.8	5.7	YJL052W	TDH1	Dehydrogenase	Carbohydrate metabolism
−1.5	13.8	YMR292W	GOT1	Membrane protein	Intracellular transport
1.1	8.7	YNL064C	YDJ1	Mitochondrial and endoplasmic reticulum import protein	Intracellular transport
−1.0	8.3	YBR164C	ARL1	ADP-ribosylation factor-like protein	Intracellular transport
5.4	7.3	YNL036W	NCE103	Involved in nonclassical protein export	Intracellular transport
2.0	5.5	YBR105C	VID24	Involved in vacuolar protein targeting	Intracellular transport

[a] The genes in cluster 1 with the largest differential in expression and which had the same expression profile as *SIT1* are sorted according to functional family. Boldface indicates genes encoding proteins involved in metal metabolism.

into Clustal groupings based on similar expression profiles over time, as assessed by standard correlation K-mean clustering using the bioinformatics software GeneSpring version 3.0, described in Materials and Methods. Six differential expression profile cluster groups were identified based on this analysis (data not shown). Cluster 1, the group with the largest number of differentially expressed ORFs (240), showed an overall increase in differential ranging from 3-fold to 30-fold at the 3-h time point (data not shown). We chose this cluster as the focus of further analysis based on the magnitude of the differentials and the presence of a majority of the differentially expressed ORFs.

Genes in cluster 1 that exhibited the greatest change in expression were sorted into functional families, a selection of which is shown in Table 1, according to classifications in the Munich Information Center for Protein Sequences (http://www.mips.biochem.mpg.de/) and the Stanford *Saccharomyces* Genome Database (http://genome-www.stanford.edu/Saccharomyces/). We were most interested in two of the functional families: detoxification and transport facilitation. ORFs in cluster 1 belonging to these two functional families are shown in the top portion of Table 1. Among these was *SIT1*, encoding an iron siderophore transporter. Several other ORFS whose products have a role in metal metabolism, such as *ARN2* and *CTR2*, were also identified. Other functional gene categories that exhibited similar temporal regulation include those encoding proteins involved in protein synthesis, carbohydrate metabolism, and intracellular transport.

Differential expression of metal acquisition ORFs. The presence of SIT1 and other metal transporter genes among the highly expressed ORFs triggered a more thorough investigation of ORFs involvd in metal transport and availability, with those involved with iron transport being of particular interest. Yeast has several mechanisms by which it acquires iron from the environment (reviewed in reference 57). In addition to *SIT1*, two additional Fe siderophore transporter geens, *TAF1*/*ARN2* and *ENB1*/*ARN4*, demonstrate significant positive differential expression at the 3-h time point (Table 1). A fourth siderophore transporter gene, *ARN1*, has a relatively steady expression level twofold that of the control (data not shown).

Though the gene for the transporter of the high-affinity elemental Fe(II) acquisition system, *FTR1*, showed no significant differences in expression, the second component of this system, *FET3*, which encodes an Fe oxidase, had a threefold increase over control values at 3 h posttreatment. In addition, two copper transporter genes, *CCC2* and *CTR2*, also showed increased expression. Copper has been demonstrated as essential for FET3 function (5, 13, 14, 63). The low-affinity *FET4*

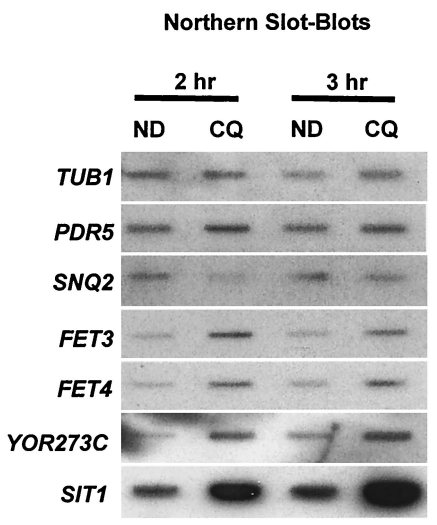

	Fold-Change by Densitometry		Fold-Change by OligoArrray	
	2 hr	3 hr	2 hr	3 hr
TUB1	0.5	1.5	-1.2	1.0
PDR5	1.2	1.4	1.4	1.7
SNQ2	-1.9	-1.0	1.3	-1.5
FET3	3.0	2.9	1.2	3.0
FET4	2.5	3.2	1.6	2.0
YOR273C	>5.0	>8.0	2.4	3.0
SIT1	>5.0	>10.0	1.7	6.0

FIG. 1. Northern slot blot analysis of selected genes. Total RNA isolated from control (ND) and CQ-treated cells at 2 and 3 h were probed with PCR-amplified labeled ORFs. Probe hybridization signals were measured with Image software. The changes between drug-treated and control cells was calculated from these densitometry measurements and are reported along with the changes calculated from the GeneChip data. *TUB1*, tubulin gene; *PDR5* and *SNQ2*, ABC transporter genes; *FET3*, Fe oxidase gene; *FET4*, Fe(III) transporter gene; *YOR273C*, transport facilitator gene; *SIT1*, iron siderophore gene.

Fe(III) transporter gene also exhibited a modest increase in expression across the course of the experiment.

A third group of genes, *SMF1* and *SMF2*, are also involved in Fe transport and are related to mammalian *NRAMP*. *SMF1* was repressed at 2 h and then returned to control levels of expression at 3 h posttreatment. *SMF2*, on the other hand, moved from a repressed state to a fourfold increase over control values at 3 h.

The transcriptional regulator gene, *AFT1*, which regulates several Fe acquisition genes (*FET3*, *FTR1*, *FRE1*, *FRE2*, *ARN1*, *TAF1*, *SIT1*, and *ENB1*) also exhibited the same peak at 3 h, though at a much more modest level.

These data taken together indicate that expression of ORFs involved in iron availability increase in response to CQ treatment. This suggests that CQ may interfere with iron uptake or availability as at least one of its modes of action.

Confirmation of expression differentials by Northern analysis. As a validation of the data produced by the GeneChip array, we performed Northern slot blot analysis on a number of individual genes. Total RNA from control and CQ-treated cells were probed with PCR-amplified labeled ORFs as described in Materials and Methods. PDR5 and SNQ1 are ATP-binding cassette (ABC) transporters in the pleiotropic drug resistance family. PDR5 deletion mutants have previously been shown to exhibit increased sensitivity to CQ. The resulting hybridization signals are shown in Fig. 1 along with the change differentials reported from the GeneChip and those calculated from densitometry analysis of the Northern hybridizations. In general, the patterns of expression obtained with the two methods correspond with one another. In the case of *SIT1* and *YOR273C*, expression appears to be somewhat underreported by the microarray analysis compared to the signal observed on the Northern blot.

CQ treatment of iron transport mutants. Yeast strains deficient in components of the iron transport pathways were tested for their sensitivity to CQ. Strains deficient in both FET3 and FET4, the high- and low-affinity elemental iron transporters, respectively, have an approximately 50% decrease in growth compared to wild-type strains in the presence of CQ (Fig. 2a). In the absence of CQ these mutants have a growth profile similar to that of wild type cells (data not shown). This differential sensitivity is not observed with strains deficient in FET3 alone (data not shown). While we have not directly tested single FET4 mutants, we suspect that they will also exhibit CQ insensitivity, since FET3 and FET4 single mutants do not exhibit defects in iron transport that are observed with FET3 FET4 double mutants (data not shown). Strains deficient in *SIT1*, encoding the iron siderophore, were also insensitive to CQ treatment, and the additional deletion of *SIT1* did not significantly alter the CQ susceptibility of FET3 FET4 double mutants (Fig. 2a). No differential sensitivity was observed with any other quinoline drug tested or with an unrelated drug, cycloheximide (Fig. 2a).

Growth of yeast on iron-depleted medium in the presence of CQ. The observation of increased CQ sensitivity in yeast genetically limited in iron acquisition (*FET3* and *FET4*) indicated that CQ might act by creating a condition of iron starvation. Iron can be limited in yeast medium by the metal chelator BPS. When plated on iron-depleted medium containing a gradient of 0 to 100 μM BPS, growth of the various yeast strains was similar to growth on a CQ gradient. Strains containing a *SIT1* deletion were not affected, but strain DEY1433, with both *FET3* and *FET4* deleted, exhibited a 60% growth reduction compared to wild-type cells (data not shown). The additional deletion of *SIT1* did not alter the growth profile under these conditions (data not shown).

To test whether yeast strains grown in a limited-iron environment exhibit elevated sensitivity to CQ, strain DEY1433 was grown on plates that were partially iron depleted by a subinhibitory concentration of BPS and also contained a subinhibitory gradient of CQ (97 mM) (Fig. 2b). Neither of these

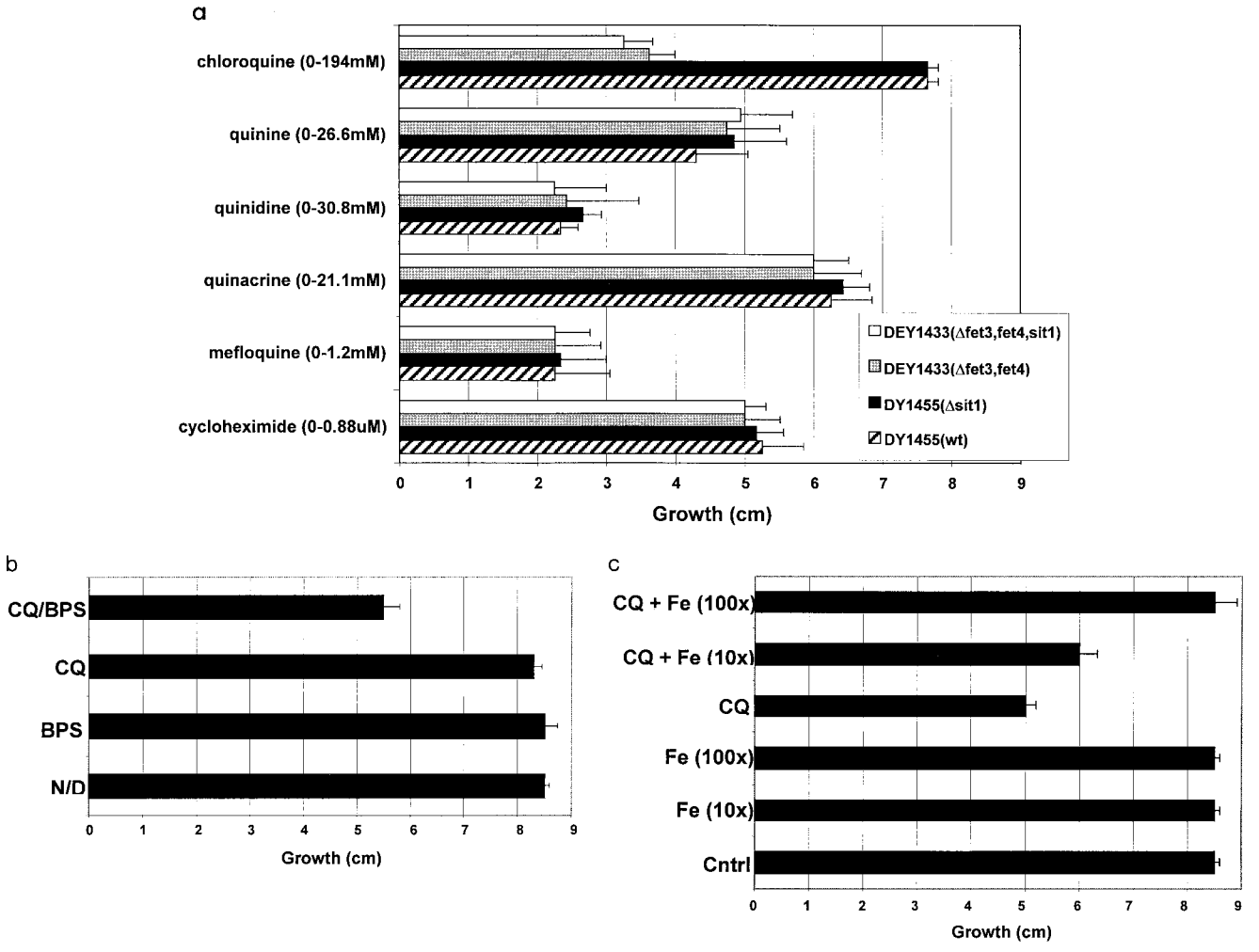

FIG. 2. (a) Growth of iron transport mutants on a battery of drug gradients. Strains DEY1455, DEY1455ΔSIT1, DEY1433, and DEY1433ΔSIT1 were plated on gradients of CQ (0 to 194 mM), quinine (0 to 26.6 mM), quinidine (0 to 30.8 mM), quinacrine (0 to 21.1 mM), mefloquine (0 to 1.2 mM), and cycloheximide (0 to 0.88 μM) as described in Materials and Methods. The plates were incubated at 30°C for 2 to 3 days, after which growth across the plates was measured. Data are the averages of at least three independent experiments. (b) Growth of yeast in presence of CQ under iron-limiting conditions. DEY1433 (ΔFET3 FET4) was plated on a continuous concentration of 20 μM BPS, a 0 to 97 mM gradient of CQ, or a combination of the two (CQ/BPS) as described in Materials and Methods. Growth across these plates was determined after incubation at 30°C for 2 to 3 days. (c) Growth of yeast in the presence of CQ under iron-supplemented conditions. DEY1433 was plated on plates containing 7.4 μM (10×) supplemental $FeCl_3$ or 74 μM (100×) $FeCl_3$, a gradient of 0 to 194 mM CQ, or a combination of both as described in Materials and Methods. Growth across these plates was determined after incubation at 30°C for 2 to 3 days.

treatments alone had much impact on growth, but in combination, they reduced growth by approximately 30%.

BPS is also known to be a copper chelator. The importance of copper in iron acquisition is noted above. To eliminate the possibility that the observed phenomenon is the result of copper depletion, we grew yeast on copper-supplemented medium in the presence of CQ. The growth of DEY1433 was unaltered by supplementation with copper in the presence or absence of CQ (data not shown).

Growth of yeast on iron-supplemented medium in the presence of CQ. To determine whether excess iron could rescue cells from CQ killing, cells were grown in different concentrations of iron, ranging from 0.74 to 74 μM, in the absence of CQ or in the presence of CQ ranging from 0 to 194 mM. Growth of DEY1433 was unaffected by excess iron in the absence of CQ (Fig. 2c). In the presence of higher iron concentrations, CQ had no effect on growth of these iron transport-deficient cells (Fig. 2c).

Iron uptake in the presence of CQ. To determine whether CQ had a direct impact on iron transport, the accumulation of $^{55}FeCl_3$ by wild-type strain DEY1455 was measured over time. In the presence of CQ, a decrease in total accumulation as well as the rate of accumulation was observed over a 6-h period (Fig. 3). Yeast cells had normal morphology with budding forms throughout the experiment (data not shown).

To determine the nature of CQ inhibition of iron uptake, we plotted velocity against substrate concentration over a range of [$^{55}FeCl_3$] (0.1 to 5.0 μM). The simple plateau curve indicated Michaelis-Menten kinetics (Fig. 4a). Double-reciprocal plots were produced from iron uptake experiments with a range of

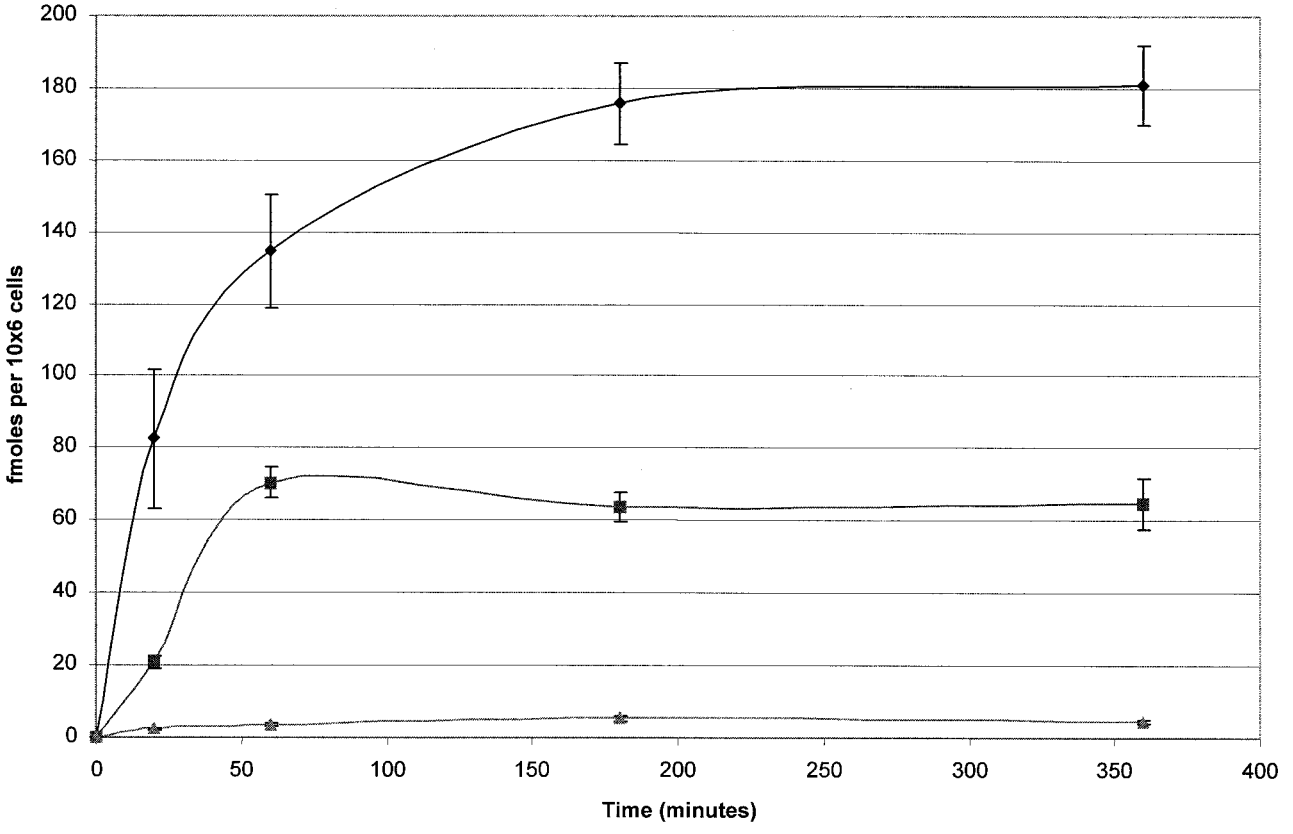

FIG. 3. Time course of $^{55}FeCl_3$ uptake by *S. cerevisiae* in the presence of CQ. Strain DEY1455 was incubated in LIM−EDTA at 30°C with 5 μM $^{55}FeCl_3$ for 6 h in the presence or absence of 9.7 and 97 mM CQ. Aliquots were precipitated onto glass fiber filters for scintillation analysis at the indicated time points. Cultures were kept in log phase over the course of the experiment by periodic dilution with LIM−EDTA containing the appropriate concentrations of $^{55}FeCl_3$ and CQ.

iron substrate (0.1 to 10 μM) and CQ (0 to 97 mM) concentrations (Fig. 4b). The apparent K_m for iron uptake by cells increased from 1.4 μM in the absence of drug to 25.7 μM at a CQ concentration of 97 mM. From these data, a K_i of 4.66 μM was calculated. The double-reciprocal plots and K_m values most closely resemble a model of competitive inhibition.

Uptake of CQ by *S. cerevisiae* in the presence of supplemental iron. To further investigate the potential interaction between CQ and iron transport, we measured [^{14}C]CQ uptake in the absence and presence of excess iron (74 μM, 100-fold excess). In these experiments, strain DEY1455 was incubated with [^{14}C]CQ for 6 h with and without supplemental iron. Samples were taken at 1, 2, 4, and 6 h, and the total [^{14}C]CQ accumulation was measured as described in Materials and Methods (Fig. 5). In contrast to iron intake, which reached saturation at around 2 h, CQ accumulation was significantly higher at the 6-h time point. Similarly, [^{14}C]CQ accumulation increased with increasing incubation time in the presence of 100-fold excess iron. In addition, total [^{14}C]CQ accumulation was equivalent for both samples at each time point.

DISCUSSION

Analysis of transcriptional profiles of CQ-treated cells demonstrated that among the genes with the largest changes in mRNA levels were a number of genes encoding transporters involved in cellular iron availability (*SIT1*, *TAF1*, *ENB1*, and *SMF2*). This response suggests that CQ toxicity may in part be due to interference with iron uptake or metabolism. In support of this, we provided evidence that yeast deprived of iron, either by gene knockout of *FET3* and *FET4* or by the presence of a chelator, demonstrated sensitivity to CQ. Furthermore, we demonstrated that CQ acts as a competitive inhibitor of iron uptake in yeast. Interestingly, a reciprocal effect was not observed when iron was used to inhibit CQ accumulation. This is not altogether surprising, since CQ, an amphiphilic compound, is able to gain entry into cells without the assistance of membrane transporters (19), and the kinetics of accumulation of iron and CQ are dramatically different (compare Fig. 4b and 5).

Several of the CQ responsive genes we identified are regulated by the iron-responsive DNA binding protein, AFT1 (61), whose gene also exhibited a similar expression pattern (data not shown). It would be of interest to directly test which of these genes might have an effect on CQ resistance, since it has been previously demonstrated that the overexpression of *YOR273c* in response to CQ treatment does not confer resistance to CQ (16).

The involvement of CQ in the disruption of iron metabolism has been noted in many biological systems including the fungus

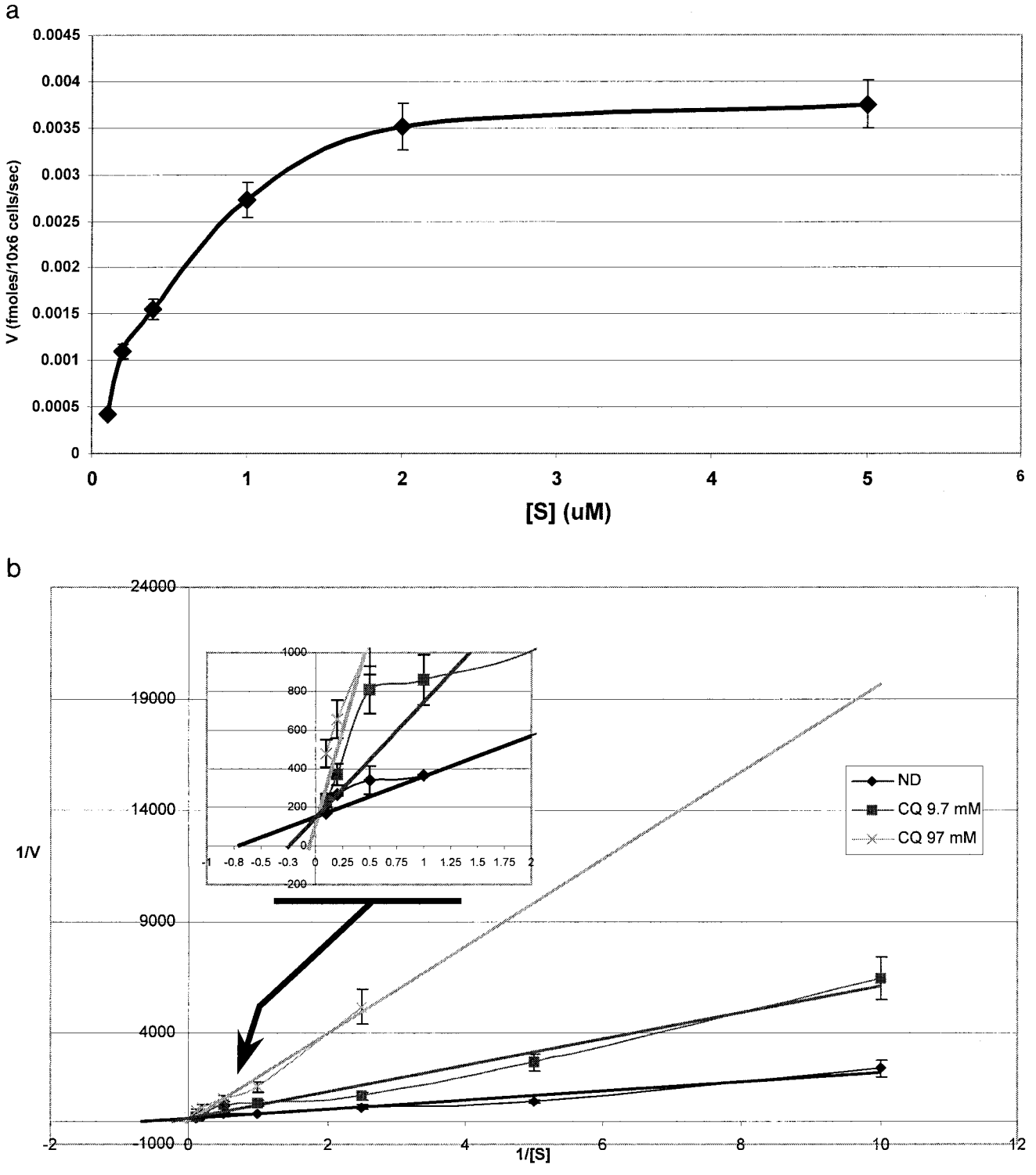

FIG. 4. (a) Lineweaver-Burk plots for $^{55}FeCl_3$ uptake by *S. cerevisiae* in the presence of CQ. Strain DEY1455 was incubated in LIM−EDTA at 30°C for 20 min in the presence of various concentrations of $^{55}FeCl_3$ (0.1 to 10.0 μM) and CQ (0.0, 9.7, and 97 mM). Samples were precipitated onto glass fiber filters for scintillation analysis. Velocity (V) is plotted against a range of [$^{55}FeCl_3$] (0.1 to 5.0 μM). (b) A double-reciprocal Lineweaver-Burk plot was created from the uptake data. The average apparent K_m, calculated as $-1/x$ intercept, for 1, 9.7, and 97 μM CQ are 1.4, 4.17, and 25.72 μM. The average apparent K_i, calculated as described in Materials and Methods, was 4.66 μM. The reported plot was derived from three independent experiments done in triplicate.

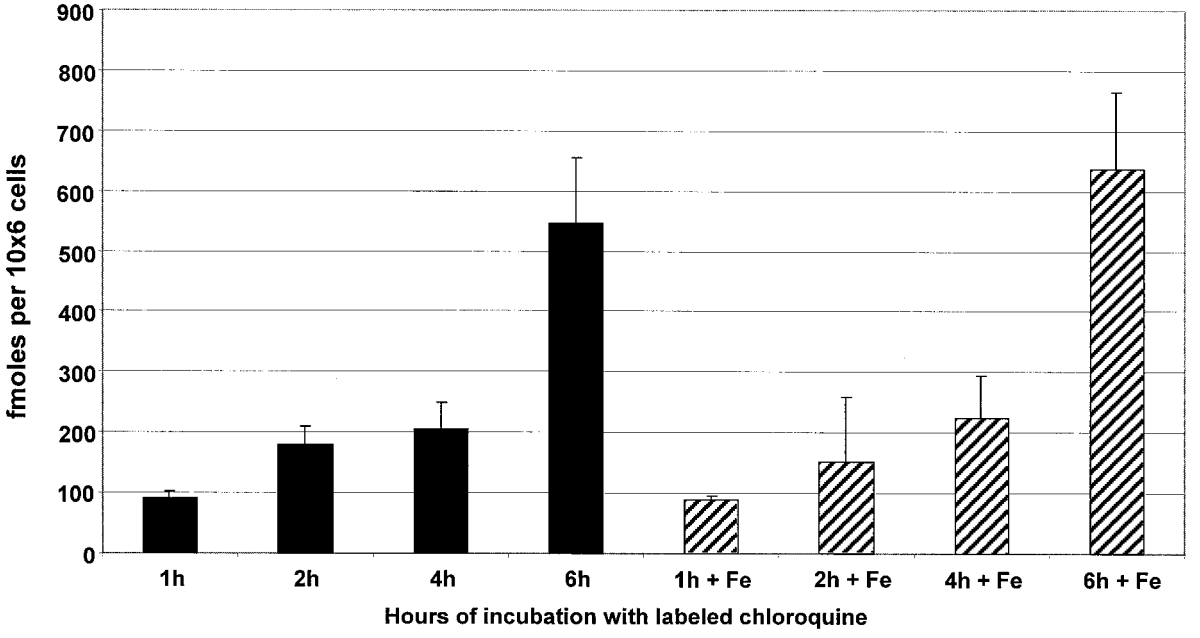

FIG. 5. Accumulation of CQ by *S. cerevisiae* in the presence of supplemental iron. Yeast strain DEY1455 was incubated at 30°C for 6 h with 50 nM [^{14}C]CQ and in the presence or absence of 74 μM $FeCl_3$ (100 times the amount in normal medium). Aliquots were taken and precipitated onto glass fiber filters for scintillation analysis at the indicated time points. Samples for each condition were incubated on ice to control for cell surface adhesion of drug. The data are the averages of at least three independent experiments.

Histoplasma capsulatum (39) and the bacteria *Francisella tularensis* (22) and *Legionella pneumophila* (9), recently reviewed by Weber et al. (56). Similar activity has been noted in a number of other cell types, including mammalian endothelial cells and macrophages (4, 6, 21, 25, 27, 28, 30, 40, 43, 52). Previous work has shown that CQ treatment can alter vacuolar pH in yeast (42). CQ concentrates in lysosomes (as much as 10,000-fold) via deprotonation and ion trapping and increases the pH of these compartments. This increase in pH then prevents the release of iron from the iron binding protein transferrin, thereby depriving the cell and associated pathogens of adequate iron. However, interrupting the release of iron from carrier proteins seems unlikely to be a primary mechanism in this system, because to date no iron carrier protein system has been identified in *S. cerevisiae*.

No such iron carrier system has been identified in *P. falciparum* either. In the *Plasmodium* parasite, CQ accumulates to millimolar concentrations in the acidic food vacuole (2, 15, 62), where it is proposed to act by interfering with the polymerization of toxic heme, thus poisoning the cells with their own waste. This process is proposed to involve the binding of CQ to heme, which is supported by spectrophotometric studies (reviewed in reference 20). Other proposed mechanisms of toxicity include inhibition of DNA replication and RNA synthesis (3, 11, 41, 53), inhibition of hemoglobin degradation (24), and lysosomotrophic activities.

The degradation of host hemoglobin by *Plasmodium* spp. provides the parasite with essential amino acids and other required nutrients, including iron. Deprivation of the iron supply by interference with hemoglobin metabolism has also been proposed as a mode of action of CQ, and the importance of iron homeostasis as a potential drug target in the parasite has been promoted by a number of groups (24, 35, 49, 60).

As with virtually all cell types, iron is an essential nutrient for the growth and proliferation of *Plasmodium* spp. (7, 23, 47, 51, 58). The genes involved in iron acquisition, trafficking, and metabolism in *Plasmodium* spp. have not yet been characterized. BLAST sequence homology searches of the database *Plasmo*DB (http://www.plasmodb.org) (44) using sequences of genes involved in iron metabolism in other organisms have resulted in the identification of only a handful of potential homologues in *Plasmodium* to date. The strongest alignments were produced with iron regulator protein homologues, ABC iron transporters, and members of the *NRAMP* family. Preliminary characterization indicates that a homologue of *NRAMP* is expressed in *P. falciparum* (David Sullivan [Johns Hopkins University], personal communication). Additionally, *FET3* and *AFT1* homologues could also be identified. Further study of these potential iron metabolism homologues in *P. falciparum* will broaden our understanding of metabolic pathways in the parasite and may shed light on new targets for pharmacological treatments of malaria.

Iron chelators, including deferoxamine, have been shown to act as antimalarials, and their use has demonstrated the potential of targeting iron homeostasis of the parasite as a drug intervention (reviewed in references 26, 46, and 50). Recent data suggest that iron chelation in *Plasmodium* spp. has detrimental effects on expression of a number of mitochondrial genes (37), influences the efficiency of the polymerization of hematin (54), and interferes with labile iron stores of both the host and parasitic cell (34). A recently published study suggests

that iron can inhibit the in vitro activities of a number of antibiotics in *P. falciparum* (45).

Our data suggest that CQ may play a role in iron metabolism, in particular as an inhibitor of iron transport. This work is based on a model system, *S. cerevisiae*, and the CQ concentrations used in this system are higher than those required to kill *P. falciparum*. However, CQ is accumulated in the parasite food vacuole to millimolar concentrations, concentrations similar to those used in these experiments, and thus, this work may have biological relevance to the in vivo parasite system (2, 15, 62). It is not clear whether the parasite acquires iron via the food vacuole, but such a mechanism has been proposed (33). Investigation of iron metabolism in *P. falciparum* in the presence and absence of CQ may provide insight into this possible mechanism. Interestingly, whole-genome expression analysis has indicated the upregulation of several uncharacterized genes in *P. falciparum* treated with CQ (A. Munasinghe, unpublished data). Perhaps some of these yet-to-be-identified genes are related to iron transport.

ACKNOWLEDGMENTS

This work was supported by Department of the Army AASERT grants DAAG55-98-1-0186 and DAMD 17-98-1-8003, and NIH R01 grant AI27872-11.

We thank the scientists and funding agencies comprising the international Malaria Genome Project for making sequence data from the genome of *P. falciparum* (3D7) public prior to publication of the completed sequence. The Sanger Centre (United Kingdom) provided sequences for chromosomes 1, 3 to 9, and 13. A consortium composed of The Institute for Genome Research, along with the Naval Medical Research Center, sequenced chromosomes 2, 10, 11 and 14. The Stanford Genome Technology Center sequenced chromosome 12. We thank Karl Kuckler (University and Biocenter of Vienna) for strain YPH499, E. Lesuisse (Institut Jacques Monod, Université Paris) for DEY1455, DEY1433, and derivatives, Wilbur Milhous and Mark Novak of Walter Reed Army Institute of Research for the [^{14}C]CQ (WR1544), and M. Wessling-Resnick, A. Dancis, D. Eide, M. Loyevsky, D. Sullivan, and A. Lailin for helpful discussions. We thank Connie Chow for her review and editing of the manuscript.

REFERENCES

1. **Adams, P. A., P. A. Berman, T. J. Egan, P. J. Marsh, and J. Silver.** 1996. The iron environment in heme and heme-antimalarial complexes of pharmacological interest. J. Inorg. Biochem. **63:**69–77.
2. **Aikawa, M.** 1972. High-resolution autoradiography of malarial parasites treated with 3 H-chloroquine. Am. J. Pathol. **67:**277–284.
3. **Allison, J. L., R. L. O'Brien, and F. E. Hahn.** 1965. DNA: reaction with chloroquine. Science **149:**1111–1113.
4. **Armstrong, N. J., and E. H. Morgan.** 1983. The effect of lysosomotrophic bases and inhibitors of transglutaminase on iron uptake by immature erythroid cells. Biochim. Biophys. Acta **762:**175–186.
5. **Askwith, C., D. Eide, A. Van Ho, P. S. Bernard, L. Li, S. Davis-Kaplan, D. M. Sipe, and J. Kaplan.** 1994. The FET3 gene of S. cerevisiae encodes a multicopper oxidase required for ferrous iron uptake. Cell **76:**403–410.
6. **Baynes, R., G. Bukofzer, T. Bothwell, W. Bezwoda, and B. Macfarlane.** 1987. Transferrin receptors and transferrin iron uptake by cultured human blood monocytes. Eur. J. Cell Biol. **43:**372–376.
7. **Becuwe, P., S. Gratepanche, M. N. Fourmaux, J. Van Beeumen, B. Samyn, O. Mercereau-Puijalon, J. P. Touzel, C. Slomianny, D. Camus, and D. Dive.** 1996. Characterization of iron-dependent endogenous superoxide dismutase of Plasmodium falciparum. Mol. Biochem. Parasitol. **76:**125–134.
8. **Bloland, P. B., and M. Ettling.** 1999. Making malaria-treatment policy in the face of drug resistance. Ann. Trop. Med. Parasitol. **93:**5–23.
9. **Byrd, T. F., and M. A. Horwitz.** 1991. Chloroquine inhibits the intracellular multiplication of Legionella pneumophila by limiting the availability of iron. A potential new mechanism for the therapeutic effect of chloroquine against intracellular pathogens. J. Clin. Investig. **88:**351–357.
10. **Chee, M., R. Yang, E. Hubbell, A. Berno, X. C. Huang, D. Stern, J. Winkler, D. J. Lockhart, M. S. Morris, and S. P. Fodor.** 1996. Accessing genetic information with high-density DNA arrays. Science **274:**610–614.
11. **Cohen, S. N., and K. L. Yielding.** 1965. Inhibition of DNA and RNA polymerase reactions by chloroquine. Proc. Natl. Acad. Sci. USA **54:**521–527.
12. **Cunningham, R. P., S. M. Saporito, S. G. Spitzer, and B. Weiss.** 1986. Endonuclease IV (nfo) mutant of *Escherichia coli*. J. Bacteriol. **168:**1120–1127.
13. **Dancis, A., D. G. Roman, G. J. Anderson, A. G. Hinnebusch, and R. D. Klausner.** 1992. Ferric reductase of Saccharomyces cerevisiae: molecular characterization, role in iron uptake, and transcriptional control by iron. Proc. Natl. Acad. Sci. USA **89:**3869–3873.
14. **Dancis, A., D. S. Yuan, D. Haile, C. Askwith, D. Eide, C. Moehle, J. Kaplan, and R. D. Klausner.** 1994. Molecular characterization of a copper transport protein in S. cerevisiae: an unexpected role for copper in iron transport. Cell **76:**393–402.
15. **de Duve, C., T. de Barsy, B. Poole, A. Trouet, P. Tulkens, and F. Van Hoof.** 1974. Lysosomotropic agents. Biochem. Pharmacol. **23:**2495–2531.
16. **Delling, U., M. Raymond, and E. Schurr.** 1998. Identification of *Saccharomyces cerevisiae* genes conferring resistance to quinoline ring-containing antimalarial drugs. Antimicrob. Agents Chemother. **42:**1034–1041.
17. **Eide, D., S. Davis-Kaplan, I. Jordan, D. Sipe, and J. Kaplan.** 1992. Regulation of iron uptake in Saccharomyces cerevisiae. The ferrireductase and Fe(II) transporter are regulated independently. J. Biol. Chem. **267:**20774–20781.
18. **Eide, D., and L. Guarente.** 1992. Increased dosage of a transcriptional activator gene enhances iron-limited growth of Saccharomyces cerevisiae. J. Gen. Microbiol. **138:**347–354.
19. **Ferrari, V., and D. J. Cutler.** 1991. Kinetics and thermodynamics of chloroquine and hydroxychloroquine transport across the human erythrocyte membrane. Biochem. Pharmacol. **41:**23–30.
20. **Foley, M., and L. Tilley.** 1998. Quinoline antimalarials: mechanisms of action and resistance and prospects for new agents. Pharmacol. Ther. **79:**55–87.
21. **Forsbeck, K., and K. Nilsson.** 1983. Iron metabolism of established human hematopoietic cell lines in vitro. Exp. Cell Res. **144:**323–332.
22. **Fortier, A. H., D. A. Leiby, R. B. Narayanan, E. Asafoadjei, R. M. Crawford, C. A. Nacy, and M. S. Meltzer.** 1995. Growth of *Francisella tularensis* LVS in macrophages: the acidic intracellular compartment provides essential iron required for growth. Infect. Immun. **63:**1478–1483.
23. **Fry, M., and J. E. Beesley.** 1991. Mitochondria of mammalian Plasmodium spp. Parasitology **102**(Pt. 1)**:**17–26.
24. **Gabay, T., M. Krugliak, G. Shalmiev, and H. Ginsburg.** 1994. Inhibition by anti-malarial drugs of haemoglobin denaturation and iron release in acidified red blood cell lysates--a possible mechanism of their anti-malarial effect? Parasitology **108:**371–381.
25. **Ghigo, D., E. Aldieri, R. Todde, C. Costamagna, G. Garbarino, G. Pescarmona, and A. Bosia.** 1998. Chloroquine stimulates nitric oxide synthesis in murine, porcine, and human endothelial cells. J. Clin. Investig. **102:**595–605.
26. **Gordeuk, V. R., P. E. Thuma, and G. M. Brittenham.** 1994. Iron chelation therapy for malaria. Adv. Exp. Med. Biol. **356:**371–383.
27. **Iacopetta, B. J., and E. H. Morgan.** 1983. The kinetics of transferrin endocytosis and iron uptake from transferrin in rabbit reticulocytes. J. Biol. Chem. **258:**9108–9115.
28. **Karin, M., and B. Mintz.** 1981. Receptor-mediated endocytosis of transferrin in developmentally totipotent mouse teratocarcinoma stem cells. J. Biol. Chem. **256:**3245–3252.
29. **Krogstad, D. J., I. Y. Gluzman, D. E. Kyle, A. M. Oduola, S. K. Martin, W. K. Milhous, and P. H. Schlesinger.** 1987. Efflux of chloroquine from Plasmodium falciparum: mechanism of chloroquine resistance. Science **238:**1283–1285.
30. **Legssyer, R., R. J. Ward, R. R. Crichton, and J. R. Boelaert.** 1999. Effect of chronic chloroquine administration on iron loading in the liver and reticuloendothelial system and on oxidative responses by the alveolar macrophages. Biochem. Pharmacol. **57:**907–911.
31. **Lesuisse, E., P. L. Blaiseau, A. Dancis, and J. M. Camadro.** 2001. Siderophore uptake and use by the yeast Saccharomyces cerevisiae. Microbiology **147:**289–298.
32. **Lesuisse, E., M. Simon-Casteras, and P. Labbe.** 1998. Siderophore-mediated iron uptake in Saccharomyces cerevisiae: the SIT1 gene encodes a ferrioxamine B permease that belongs to the major facilitator superfamily. Microbiology **144:**3455–3462.
33. **Loria, P., S. Miller, M. Foley, and L. Tilley.** 1999. Inhibition of the peroxidative degradation of haem as the basis of action of chloroquine and other quinoline antimalarials. Biochem. J. **339:**363–370.
34. **Loyevsky, M., C. John, B. Dickens, V. Hu, J. H. Miller, and V. R. Gordeuk.** 1999. Chelation of iron within the erythrocytic Plasmodium falciparum parasite by iron chelators. Mol. Biochem. Parasitol. **101:**43–59.
35. **Mabeza, G. F., G. Biemba, and V. R. Gordeuk.** 1996. Clinical studies of iron chelators in malaria. Acta Haematol. **95:**78–86.
36. **Memisoglu, A., and L. Samson.** 2000. Contribution of base excision repair, nucleotide excision repair, and DNA recombination to alkylation resistance of the fission yeast *Schizosaccharomyces pombe*. J. Bacteriol. **182:**2104–2112.
37. **Moormann, A. M., P. A. Hossler, and S. R. Meshnick.** 1999. Deferoxamine effects on Plasmodium falciparum gene expression. Mol. Biochem. Parasitol. **98:**279–283.
38. **Nau, M. E., L. R. Emerson, R. K. Martin, D. E. Kyle, D. F. Wirth, and M. Vahey.** 2000. Technical assessment of the Affymetrix yeast expression Gene-

Chip YE6100 platform in a heterologous model of genes that confer resistance to antimalarial drugs in yeast. J. Clin. Microbiol. **38:**1901–1908.
39. **Newman, S. L., L. Gootee, G. Brunner, and G. S. Deepe.** 1994. Chloroquine induces human macrophage killing of Histoplasma capsulatum by limiting the availability of intracellular iron and is therapeutic in a murine model of histoplasmosis. J. Clin. Investig. **93:**1422–1429.
40. **Octave, J. N., Y. J. Schneider, P. Hoffmann, A. Trouet, and R. R. Crichton.** 1979. Transferrin protein and iron uptake by cultured rat fibroblasts. FEBS Lett. **108:**127–130.
41. **Parker, F. S., and J. L. Irvin.** 1952. The interaction of chloroquine with nucleic acids and nucleoproteins. J. Biol. Chem. **199:**897–909.
42. **Pearce, D. A., C. J. Carr, B. Das, and F. Sherman.** 1999. Phenotypic reversal of the btn1 defects in yeast by chloroquine: a yeast model for Batten disease. Proc. Natl. Acad. Sci. USA **96:**11341–11345.
43. **Picot, S., F. Peyron, A. Donadille, J. P. Vuillez, G. Barbe, and P. Ambroise-Thomas.** 1993. Chloroquine-induced inhibition of the production of TNF, but not of IL-6, is affected by disruption of iron metabolism. Immunology **80:**127–133.
44. **The Plasmodium Genome Database Collaborative.** 2001. *Plasmo*DB. An integrative database of the Plasmodium falciparum genome. Tools for accessing and analyzing finished and unfinished sequence data. Nucleic Acids Res.**29:**66–69.
45. **Pradines, B., C. Rogier, T. Fusai, J. Mosnier, W. Daries, E. Barret, and D. Parzy.** 2001. In vitro activities of antibiotics against *Plasmodium falciparum* are inhibited by iron. Antimicrob. Agents Chemother. **45:**1746–1750.
46. **Rosenthal, P. J., and S. R. Meshnick.** 1996. Hemoglobin catabolism and iron utilization by malaria parasites. Mol. Biochem Parasitol. **83:**131–139.
47. **Rubin, H., J. S. Salem, L. S. Li, F. D. Yang, S. Mama, Z. M. Wang, A. Fisher, C. S. Hamann, and B. S. Cooperman.** 1993. Cloning, sequence determination, and regulation of the ribonucleotide reductase subunits from Plasmodium falciparum: a target for antimalarial therapy. Proc. Natl. Acad. Sci. USA **90:**9280–9284.
48. **Sambrook, J., E. F. Fritsch, and T. Maniatis.** 1989. Molecular cloning: a laboratory manual, 2nd ed. Cold Spring Harbor Laboratory Press, Plainview, N.Y.
49. **Siu, P. M.** 1972. Malaria: the effect of iron and chloroquine on the erythrocytic forms of Plasmodium berghei. Proc. Soc. Exp. Biol. Med. **139:**799–802.
50. **Smith, H. J., and M. Meremikwu.** 2000. Iron chelating agents for treating malaria. Cochrane Database Syst. Rev. **2:**CD001474.
51. **Surolia, N., and G. Padmanaban.** 1992. De novo biosynthesis of heme offers a new chemotherapeutic target in the human malarial parasite. Biochem. Biophys. Res. Commun. **187:**744–750.
52. **Swaiman, K. F., and V. L. Machen.** 1986. Chloroquine reduces neuronal and glial iron uptake. J. Neurochem. **46:**652–654.
53. **Thelu, J., J. Burnod, V. Bracchi, and P. Ambroise-Thomas.** 1994. Identification of differentially transcribed RNA and DNA helicase-related genes of Plasmodium falciparum. DNA Cell Biol.**13:**1109–1115.
54. **Vippagunta, S. R., A. Dorn, A. Bubendorf, R. G. Ridley, and J. L. Vennerstrom.** 1999. Deferoxamine: stimulation of hematin polymerization and antagonism of its inhibition by chloroquine. Biochem. Pharmacol. **58:**817–824.
55. **Vippagunta, S. R., A. Dorn, H. Matile, A. K. Bhattacharjee, J. M. Karle, W. Y. Ellis, R. G. Ridley, and J. L. Vennerstrom.** 1999. Structural specificity of chloroquine-hematin binding related to inhibition of hematin polymerization and parasite growth. J. Med. Chem. **42:**4630–4639.
56. **Weber, S. M., S. M. Levitz, and T. S. Harrison.** 2000. Chloroquine and the fungal phagosome. Curr. Opin. Microbiol. **3:**349–353.
57. **Wessling-Resnick, M.** 1999. Biochemistry of iron uptake. Crit. Rev. Biochem. Mol. Biol. **34:**285–314.
58. **Wilson, C. M., A. B. Smith, and R. V. Baylon.** 1996. Characterization of the delta-aminolevulinate synthase gene homologue in P. falciparum. Mol. Biochem. Parasitol. **75:**271–276.
59. **Wodicka, L., H. Dong, M. Mittmann, M. H. Ho, and D. J. Lockhart.** 1997. Genome-wide expression monitoring in Saccharomyces cerevisiae. Nat. Biotechnol. **15:**1359–1367.
60. **Wyler, D. J.** 1992. Bark, weeds, and iron chelators—drugs for malaria. N. Engl. J. Med. **327:**1519–1521.
61. **Yamaguchi-Iwai, Y., R. Stearman, A. Dancis, and R. D. Klausner.** 1996. Iron-regulated DNA binding by the AFT1 protein controls the iron regulon in yeast. EMBO J. **15:**3377–3384.
62. **Yayon, A., Z. I. Cabantchik, and H. Ginsburg.** 1984. Identification of the acidic compartment of Plasmodium falciparum-infected human erythrocytes as the target of the antimalarial drug chloroquine. EMBO J. **3:**2695–2700.
63. **Yuan, D. S., R. Stearman, A. Dancis, T. Dunn, T. Beeler, and R. D. Klausner.** 1995. The Menkes/Wilson disease gene homologue in yeast provides copper to a ceruloplasmin-like oxidase required for iron uptake. Proc. Natl. Acad. Sci. USA **92:**2632–2636.